

New Insights with XRISM & Cloudy: A novel Column Density Diagnostic

Chamani M. Gunasekera¹, Peter A. M. van Hoof², Masahiro Tsujimoto³, and Gary J. Ferland⁴

¹ Space Telescope Science Institute, 3700 San Martin Drive, Baltimore, MD 21218, USA

² Royal Observatory of Belgium, Ringlaan 3, B-1180 Brussels, Belgium

³ Institute of Space and Astronautical Science (ISAS), Japan Aerospace Exploration Agency (JAXA), 3-1-1 Yoshinodai, Chuo-ku, Sagamihara, Kanagawa 252-5210, Japan

⁴ University of Kentucky, 506 Library Drive, Lexington, KY 40506, USA
e-mail: cgunasekera@stsci.edu

Received November 22, 2024 / Accepted January 18, 2024

ABSTRACT

Aims. We present a simple, yet powerful column density diagnostic for plasmas enabled by X-ray microcalorimeter observations.

Methods. With the recent developments of the spectral simulation code CLOUDY, inspired by the high spectral resolution of the X-Ray Imaging and Spectroscopy Mission (XRISM) and the Advanced Telescope for High Energy Astrophysics (Athena), we make predictions for the intensity ratio of the resolved fine-structure lines Ly α_1 and Ly α_2 of H-like ions.

Results. We show that this ratio can be observationally constrained and used as a plasma column density indicator. We demonstrate this with a XRISM observation of the high-mass X-ray binary Centaurus X-3.

Conclusions. This diagnostic is useful for a wide range of X-ray emitting plasmas, either collisionally or radiatively ionized.

Key words. atomic processes – radiative transfer – X-rays: binaries

1. Introduction

Spectral resolution is a primary limiting factor in studying the Universe's hottest phenomena. The X-Ray Imaging and Spectroscopy Mission (XRISM; Tashiro et al. 2020) launched in 2023 is poised to unlock new insights into the fundamental nature of the X-ray universe, with its state-of-the-art Resolve microcalorimeter spectrograph (Ishisaki et al. 2022). However, we will need new tools to fully use the XRISM data as it will be able to resolve many spectral features for the first time. One of them is the fine-structure doublet of the Lyman α line of H-like ions; i.e., the $2p^2P_{3/2} \rightarrow 1s^2S_{1/2}$ and $2p^2P_{1/2} \rightarrow 1s^2S_{1/2}$ transitions. We hereafter call them Ly α_1 and Ly α_2 , respectively, and discuss their line intensity ratio.

CLOUDY (last reviewed by Chatzikos et al. 2023; Gunasekera et al. 2023) is one of the most widely used spectral simulation codes, for plasmas in non-local thermodynamic equilibrium. CLOUDY handles one- and two-electron systems with a consistent method along iso-sequences. The two-electron iso-sequence with optical emission lines was expanded in Porter et al. (2012, 2013), while the code uses atomic databases for the many-electron systems (Lykins et al. 2015; Gunasekera et al. 2022). Recent work, described in Gunasekera et al. (2024), has expanded the one-electron systems to simulate X-ray spectra matching the resolution of current and future microcalorimeter observations. The detailed microphysics required to resolve the Lyman series doublet, at the resolution of XRISM, is presented in Gunasekera et al. (2024). This development will be the primary component of the CLOUDY 2025 release.

The resolving power (R) required to separate the Lyman series doublet is shown for abundant elements in Figure 1. The energy split of fine-structure levels stems from the spin-orbit

coupling term of the Hamiltonian, which increases as a function of the atomic number (Z) at a rate $\Delta E \propto Z^4$. As detailed in Gunasekera et al. (2024) the required resolving power $R = E/\Delta E \propto Z^{-2}$ becomes less demanding for higher Z elements. All high-resolution X-ray spectrometers before XRISM — the Chandra Low and the High Energy Transmission Gratings (LETG Brinkman et al. 2000; HETG Canizares et al. 2005) and the Reflection Grating Spectrometer (RGS) (Den Herder et al. 2001) onboard the X-ray Multi-Mirror Mission Newton (XMM-Newton)— are based on dispersion spectrometry, which has a spectral resolution approximately constant in wavelengths $\Delta\lambda$, thus $R = \lambda/\Delta\lambda \propto E^{-1} \propto Z^{-2}$. The resolution of the dispersion spectrometers and that required to resolve fine-structure levels have the same dependence on E by coincidence. As a result, none of the Lyman series doublets for any Z was resolved by these spectrometers.

The X-ray microcalorimeter onboard XRISM uses an entirely different spectroscopic technique based on non-dispersive X-ray microcalorimetry, whose resolution is approximately constant in energy ΔE , thus $R \propto E^1$. For $Z \geq 18$ (Ar), the Ly α doublet is resolved with XRISM for the first time for any astronomical source at a redshift of approximately zero, except for the Sun. It can even resolve the Ly β doublet for $Z \geq 26$ (Fe). This is also the case for other fine-structure levels such as He-like ions' x and y lines of the He α ($n = 2 \rightarrow 1$) transitions. For He-like ions, we denote w , x , y , and z , respectively for the $^1P_1 \rightarrow ^1S_0$, $^3P_2 \rightarrow ^1S_0$, $^3P_1 \rightarrow ^1S_0$, and $^3S_1 \rightarrow ^1S_0$ transitions from the $1s2p$ or $1s2s$ levels to the $1s^2$ ground state.

In this Letter, we focus on the Ly α doublet. We will show that the intensity ratio of the doublet is a useful diagnostic of the physical conditions of X-ray emitting plasmas. We present the theoretical predictions made by CLOUDY in Section 2 and ap-

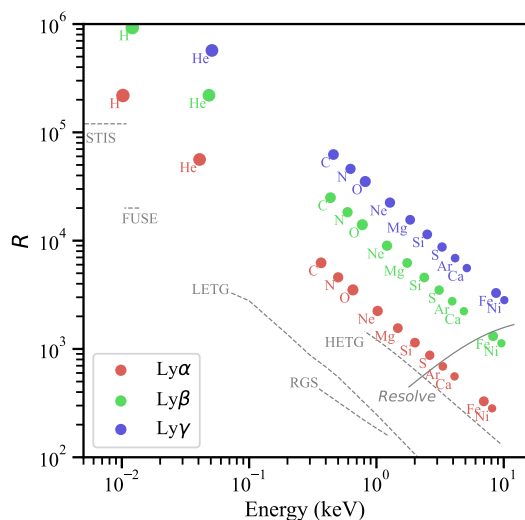


Fig. 1. Required resolving power ($R \equiv E/\Delta E$) to separate the $\text{Ly}\alpha_{1,2}$ (red), $\beta_{1,2}$ (green), and $\gamma_{1,2}$ (blue) fine-structure doublets of major elements compared to the instrumental resolving power of Hubble Space Telescope Imaging Spectrograph (STIS) (Kimble et al. 1998), Far Ultraviolet Spectroscopic Explorer (FUSE) (Moos et al. 2000), Chandra LETG (Brinkman et al. 2000) and HETG (Canizares et al. 2005), XMM-Newton RGS (Den Herder et al. 2001), and XRISM Resolve (Ishisaki et al. 2022) using the full-width half maximum (FWHM). The elements below the curves can be resolved with the spectrometer. The symbol size represents the logarithm of the solar abundance of the elements (Anders & Grevesse 1989).

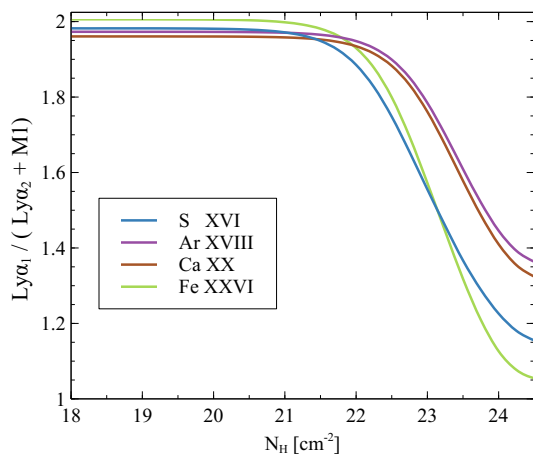


Fig. 2. Line intensity ratio of the $\text{Ly}\alpha$ doublet for selected H-like ions as a function of the plasma column density calculated with CLOUDY. Note that the absolute value of N_{H} changes for different plasma environments, as the line optical depth is converted into N_{H} using the chemical abundance, charge and level populations of the simulation. CLOUDY provides $\text{Ly}\alpha_2 + \text{M1}$ as a "blend" for Fe XXVI only. For the other one-electron species, these line must be obtained separately in CLOUDY and summed by hand.

ply the method to actual observational data with XRISM in Section 3.

2. Spectral Simulations Using Cloudy

We present a CLOUDY simulation for the plasma at the Perseus Cluster core (Aharonian et al. 2016). Being one of the brightest galaxy clusters observed in X-rays, it provides an ideal case to explore the physics. The model assumes a collisionally-ionized

plasma at a constant temperature of 4.7×10^7 K and hydrogen density of $10^{-1.5} \text{ cm}^{-3}$ with varying plasma thickness in the line of sight evaluated as the H-equivalent column density (N_{H}). We also include a microturbulent velocity of 150 km s^{-1} , ensuring more realistic line shielding and pumping.

The line radiative transport is handled using a unified approach with the goal of having a single class (a group of objects in the code that share the same properties and behaviours) in CLOUDY with the appropriate atomic parameters. Line transfer is handled within this framework. As summarized by Hummer (1962), four cases can be identified depending on the lifetimes of the upper and lower states and the importance of Doppler and radiative broadening. Kalkofen (1987) gives further details. By default, CLOUDY assumes partial redistribution for resonance lines and complete redistribution for subordinate lines. These assumptions can be changed with options in the user interface although tests show that these do not influence the conclusions presented here.

Figure 2 shows how the intensity ratio of the $\text{Ly}\alpha$ doublet changes as N_{H} increases for some selected elements. Two simple limits are apparent. At low column densities, where the line optical depth is small, the line photons escape freely without interactions. CLOUDY $\text{Ly}\alpha_j$ intensities are proportional to the populations of the upper levels, which are assumed to be proportional to their statistical weights (further discussed in Gunasekera et al. 2024). Hence the ratio is predicted to be 2 : 1 with the $\text{Ly}\alpha_1$ line being stronger. This is close to the value observed in the Fe xxvi doublet in the corona X-rays in the Sun, in which the lines are optically thin (Tanaka 1986).

As the optical depth increases, line photons undergo an increasing number of absorptions and re-emissions before escaping. As a result, the photons we observe at Earth will have the physical conditions imprinted on them where they were last re-emitted. In other words, the line flux will be determined by the physical conditions at that point. More quantitatively, this can be understood by looking at the Eddington-Barbier approximation, which states that the emergent flux is determined by the source function at the location where the line optical depth τ reaches $2/3$ when integrated from the observers point of view (Rutten 2003). Assuming the conditions are sufficiently similar in the regions where the $\text{Ly}\alpha_1$ and $\text{Ly}\alpha_2$ lines reach $\tau = 2/3$, the $\text{Ly}\alpha_1/\text{Ly}\alpha_2$ line ratio will approach 1:1 for high column densities. Note that CLOUDY does not code the Eddington-Barbier approximation explicitly, but rather uses the escape probability formalism to compute the line fluxes. This should, however, give very similar results. This implies that the $\text{Ly}\alpha$ doublet intensity ratio is sensitive to column densities in the range of $\approx 10^{20} - 10^{24} \text{ cm}^{-2}$ with different ranges for different elements, which is the appropriate range observed in many systems.

3. Observational Demonstration using XRISM

We demonstrate the proposed diagnostic using actual observation data with XRISM. We take Centaurus X-3 (Cen X-3) as an example. Cen X-3 is an eclipsing high-mass X-ray binary comprised of a neutron star (NS) and an O6.5 II-III star (Schreier et al. 1972). The X-ray spectra during eclipses are not contaminated by the direct emission from the NS, upon which absorption features are imprinted. Therefore, it is more suitable for the emission line ratio diagnostics focusing on the diffuse emission from the photoionized plasma.

Cen X-3 was observed with Resolve on February 12–15, 2024 (sequence number 300003010; Mochizuki et al. 2024). Two eclipses were covered during the XRISM observation. We

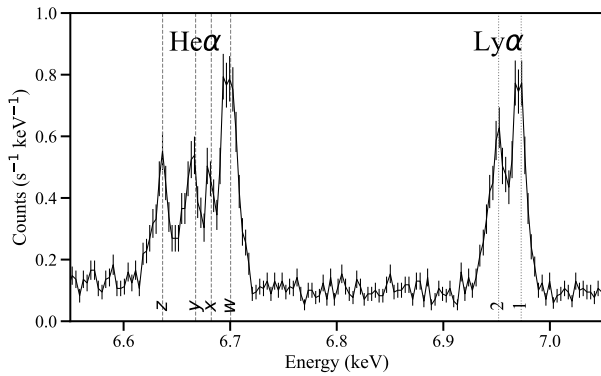


Fig. 3. Resolve spectrum of Cen X-3 during eclipse (Pradhan & Tsujimoto 2024) of Fe xxv He α and Fe xxvi Ly α complex. The fine-structure levels of the complexes are clearly resolved.

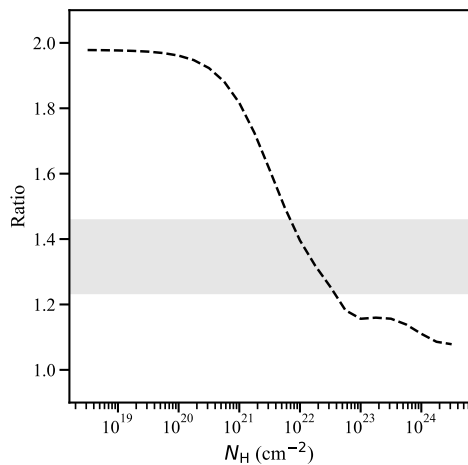


Fig. 4. Ly α_1 /Ly α_2 ratio calculated with CLOUDY for the Cen X-3 setting (dashed curve) and the observed ratio (shaded area). Though minor for this setup, the M1 transition $(2s)^2S_{1/2} \rightarrow (1s)^2S_{1/2}$ intensity is added to Ly α_2 , which cannot be resolved with Resolve.

integrated the X-ray spectrum over the eclipses for 48 ks (Figure 3). The fine-structure levels in the He α and Ly α complexes are indeed resolved. The Ly α line complex was fitted using two Gaussian lines plus a power law model to account for the underlying continuum. The line centers were fixed to the values in the APED database (Smith et al. 2001) but they were allowed to shift collectively to account for possible systematic velocities and energy gain calibration uncertainty. The line intensities were fitted individually. The widths of the two lines (1 and 2) were assumed to be the same and they were fitted simultaneously. A successful fit was obtained with a reduced $\chi^2 < 1.2$ and the line ratio was derived as 1.35 ± 0.11 .

We now apply the diagnostics proposed in Section 2. We ran a CLOUDY simulation customized for Cen X-3. The photoionizing emission is provided by the NS, which is represented by a power law of a photon index of -1.8 and a luminosity $L_X = 10^{37}$ erg s $^{-1}$ in the 1–1000 Ryd range as derived from the data. The emission lines from the photo-ionized plasma are observed when the NS is eclipsed by the O star, indicating that the plasma size is no smaller than the radius of the O star ($12 R_\odot$). We thus set the inner radius $r_{in} = 10^{12}$ cm. The ionization parameter $\log \xi \sim 4$ from the line intensity ratio of H-like versus He-like ions. These yield the electron density $n = L_X/(r_{in}^2 \xi) = 10^9$ cm $^{-3}$.

We assumed a plane-parallel geometry. The turbulent velocity was set to zero. Figure 4 shows the result. We constrain the hydrogen-equivalent column density of the plasma to be $\sim 2 \times 10^{22}$ cm $^{-2}$. This is consistent with other methods such as the He α z/w ratio (Chakraborty et al. 2021) within a factor of a few, verifying the validity of this diagnostic.

4. Summary

The present study highlights the groundbreaking potential for new science that can be uncovered by using the latest CLOUDY developments to understand microcalorimeter observations. The column thickness in the line of sight is a crucial quantifier of the X-ray emitting plasma in all systems. We presented a novel column density diagnostic using the intensity ratio of the resolved Ly α doublet of one-electron atoms, which changes from 2 to 1 as the optical thickness of the line center increases as N_H increases. Different elements have sensitivity in different ranges of the N_H for their differences in abundance, charge and level populations, oscillator strength, line profiles, and so on, which can be calculated or taken into account in CLOUDY simulations. We demonstrated this for Cen X-3 using the Fe xxvi Ly α doublet resolved with XRISM data and the CLOUDY simulation and constrained its N_H value.

Data availability

All CLOUDY models and subsequent figures used in the present paper are available at <https://gitlab.nublado.org/cloudy/papers/-/tree/main/arXiv.2411.15357>.

Acknowledgements. CMG and GJF were supported by JWST-AR-06419 and JWST-AR-06428. This research made use of the JAXA's high-performance computing system JSS3.

References

- Aharonian, F., Akamatsu, H., Akimoto, F., et al. 2016, *Nature*, 535, 117
- Anders, E. & Grevesse, N. 1989, *Geochimica et Cosmochimica Acta*, 53, 197
- Brinkman, A. C., Gunsing, T., Kaastra, J. S., et al. 2000, *Proc. of SPIE*, 4012, 81
- Canizares, C. R., Davis, J. E., Dewey, D., et al. 2005, *PASP*, 117, 1144
- Chakraborty, P., Ferland, G. J., Chatzikos, M., Guzmán, F., & Su, Y. 2021, *ApJ*, 912, 26
- Chatzikos, M., Bianchi, S., Camilloni, F., et al. 2023, *Rev. Mexicana Astron. Astrofis.*, 59, 327
- Den Herder, J. W., Brinkman, A. C., Kahn, S. M., et al. 2001, *A&A*, 365, L7
- Gunasekera, C. M., Chatzikos, M., & Ferland, G. J. 2022, *Astronomy*, 1, 255
- Gunasekera, C. M., van Hoof, P. A. M., Chatzikos, M., & Ferland, G. J. 2023, *Research Notes of the American Astronomical Society*, 7, 246
- Gunasekera, C. M., van Hoof, P. A. M., Chatzikos, M., & Ferland, G. J. 2024, *arXiv e-prints*, arXiv:2412.01606
- Hummer, D. G. 1962, *MNRAS*, 125, 21
- Ishisaki, Y., Kelley, R. L., Awaki, H., et al. 2022, *Space Telescopes and Instrumentation 2022: Ultraviolet to Gamma Ray*, 12181, 409
- Kalkofen, W. 1987, *Numerical radiative transfer*
- Kimble, R. A., Woodgate, B. E., Bowers, C. W., et al. 1998, *ApJ*, 492, L83
- Lykins, M. L., Ferland, G. J., Kisielius, R., et al. 2015, *ApJ*, 807, 118
- Mochizuki, Y., Tsujimoto, M., Kelley, R. L., et al. 2024, *ApJL*, 977, L21
- Moos, H. W., Cash, W. C., Cowie, L. L., et al. 2000, *ApJ*, 538, L1
- Porter, R. L., Ferland, G. J., Storey, P. J., & Detisch, M. J. 2012, *MNRAS*, 425, L28
- Porter, R. L., Ferland, G. J., Storey, P. J., & Detisch, M. J. 2013, *MNRAS*, 433, L89
- Pradhan, P. & Tsujimoto, M. 2024, *Bulletin de la Société Royale des Sciences de Liège*
- Rutten, R. J. 2003, *Radiative Transfer in Stellar Atmospheres*
- Schreier, E., Levinson, R., Gursky, H., et al. 1972, *ApJ*, 172, L79
- Smith, R. K., Brickhouse, N. S., Liedahl, D. A., & Raymond, J. C. 2001, *ApJ*, 556, L91
- Tanaka, K. 1986, *PASJ*, 38, 225
- Tashiro, M. S., Maejima, H., Toda, K., et al. 2020, *Space Telescopes and Instrumentation 2020: Ultraviolet to Gamma Ray*, 11444, 176